A theoretical study on the ionization of tetrachloroethylene with analysis of vibrational structure of the photoelectron spectra

Kouichi Takeshita
Faculty of Bioindustry, Tokyo University of Agriculture, Abashiri, Hokkaido 099-24, Japan

(Received 31 August 1994; accepted 9 March 1995)

Ab initio calculations have been performed to study the molecular structures and the vibrational levels of the low-lying eight ionic states ($^2B_{2u}$, $^2B_{2g}$, ^2A_u, $^2B_{3u}$, $^2B_{1g}$, ^2A_g, $^2B_{1u}$, and $^2B_{3g}$) of tetrachloroethylene. The equilibrium molecular structures and vibrational modes of these states are presented. The theoretical ionization intensity curves including the vibrational structures of the low-lying eight ionic states are also presented and compared with the photoelectron spectrum. Some new assignments of the photoelectron spectra are proposed. © *1995 American Institute of Physics.*

I. INTRODUCTION

The electronic configuration of the ground state of tetrachloroethylene is represented by a $...(2b_{3g})^2\ (9a_g)^2\ (8b_{1u})^2\ (2b_{1g})^2\ (7b_{3u})^2\ (2a_u)^2\ (7b_{2g})^2(3b_{2u})^2$ with the D_{2h} symmetry group by using the coordinate axis illustrated in Fig. 1.

The photoelectron (PE) spectroscopy investigations of tetrachloroethylene have been reported.[1–3] Between 9 and 14 eV, many bands were observed. The first band found at 9.4 eV had a vibrational structure. An interpretation of the vibrational structure was reported by Lake and Thompson.[1] The second band was found at 11.37 eV. In the 12–13 eV region, several peaks were observed. They found the six peaks at 12.18, 12.44, 12.54, 12.67, 12.77, and 12.91 eV. The band at 13.48 eV was accompanied by a vibrational structure. Lake and Thompson attempted an assignment of the vibrational energy.

Ab initio calculations on the vertical ionization energies have been reported to assign the electronic states of these band.[2,3] In the 9–14 eV region, eight electronic states should contribute to the spectrum. However, some assignments have not been established in the 12–13 eV region, because several states were predicated to be close together.

The position of a band depends on the adiabatic ionization energy and the shape of a band depends on the vibrational structure. As a molecule is ionized, the equilibrium molecular structure and the character of the vibrational mode should change from those of the ground state. The ionization energy and vibrational structure of the PE spectrum reflect these changes. It is significant to investigate the ionization energy and vibrational structure associated with the change in the equilibrium molecular structure and the vibrational mode by ionization.

No theoretical investigation on the molecular structures and the vibrational levels of the ionic states have been reported. In this work, we determine the equilibrium molecular structures of the ground and lower eight ionic states ($^2B_{2u}$, $^2B_{2g}$, ^2A_u, $^2B_{3u}$, $^2B_{1g}$, ^2A_g, $^2B_{1u}$, and $^2B_{3g}$) by using the *ab initio* self-consistent field (SCF) method. Within the framework of the adiabatic approximation and the harmonic oscillator approximation, we calculate the harmonic force constant matrix elements over variables of the totally symmetric distortion and the vibrational frequencies of the three totally symmetric modes. We obtain an approximate theoretical intensity curve using the Franck–Condon factor (FCF), which is given by the square of the overlap integrals between the vibrational wave function of the ground state and that of the ionic state. Based on these calculations, we discuss an assignment of the electronic state and vibrational structure of the band compared to the photoelectron spectrum.

II. METHOD OF CALCULATIONS

We use the basis sets of the MIDI-4-type prepared by Tatewaki and Huzinaga.[4] These are augmented by one p-type polarization function for H and one d-type polarization function for C and Cl. The exponents of the polarization function for H, C, and Cl are 0.68, 0.61, and 0.56, respectively.

The gradient technique for the Roothaan's restricted Hartree–Fock (RHF) method is applied to find the optimum molecular structures of the ground and ionic states.

The single and double excitation configuration interaction (SDCI) method is used to obtain more accurate values of the vertical ionization (VI) and adiabatic ionization (AI) energies. A single reference configuration of the RHF wave function of the respective state is used. In the SDCI method, singly and doubly excited configuration state functions (CSFs) are generated where the inner shells are kept frozen. The generated CSFs are then restricted to the first-order interacting space.[5] Because the dimensions of the CI are too large for our computer program system, we adopt a CSF selection process by the second-order perturbation theory. The number of the generated CSFs is reduced from about 73 000 to 21 000. We estimate the total energy including the contribution from the rejected CSFs by a second-order perturbation theory.[6]

The harmonic force constant matrix elements are calculated by the gradient technique with the RHF wave function; the second derivative is estimated by the numerical differentiation of the analytically calculated first derivative. We calculate the FCFs of only the totally symmetric vibrational modes. In calculating FCFs, we approximate the vibrational wave functions by those obtained by the harmonic oscillator model. We assume that the initial state is the zero point vibrational level of the ground state. The method of calculation

 0021-9606/95/102(22)/8922/8/$6.00

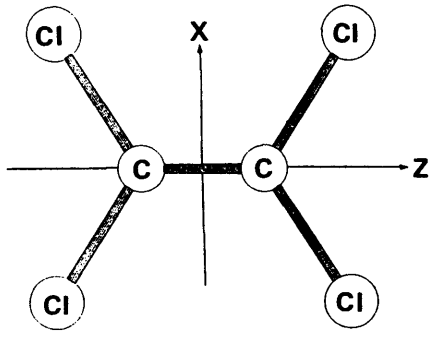

FIG. 1. A definition of the coordinate axis.

of the FCF and theoretical intensity curves is the same as we used in the previous paper.[7]

This work is carried out by using the computer program system GRAMOL[8] for the gradient technique and the calculation of normal modes, and MICA3[9] for the CI calculations.

III. RESULTS AND DISCUSSION

For the ground state of ^1A_g, the optimized geometrical parameters are shown in Table I, which are in good agreement with the experimental ones.[10] The vibrational frequencies are shown in Table II. The frequencies are arranged in order of magnitude. Comparing with the observed values[11] of the ground state, we overestimate the frequencies by 6.7%–16.2%. Each vibrational mode is characterized by using the conventional potential energy distribution (PED) and the classical half-amplitude of the zero point vibrational levels. Table III shows the PED, which is described using the totally symmetrical displacement coordinate. The classical half-amplitude is shown in Table IV. Table III shows that the ν_1 and ν_2 modes of the ^1A_g state are characterized mainly as the C=C and C–Cl stretching motions, respectively. It also shows that the C–Cl and C=C stretching motions contribute to the ν_1 and ν_2 modes, respectively. It is found from Table IV that the characters of the ν_1 and ν_2 modes are the mixtures of the C=C and C–Cl stretching motions. The C=C and C–Cl stretching motions couple with the out-of-phase mode in ν_1 and with the in-phase mode in ν_2. The ν_3 mode is interpreted as the C=C–Cl bending motion. We notice from Table IV that the amplitude of the C=C–Cl bending motion of the ν_1 mode is as large as that of the ν_3 mode.

For the ionic states, Tables I–IV also show the optimized geometric parameters, vibrational frequencies, conventional potential energy distributions, and classical half-amplitudes of the zero point vibrational levels, respectively. Table I also includes the magnitude of the change in the equilibrium molecular structure by ionization. It is found from Table IV that the classical half-amplitude of the zero point vibrational levels of the C=C, C–Cl stretching and C=C–Cl bending mo-

TABLE I. Optimized molecular structure and magnitude of the change in the geometry by ionization.[a]

State	C=C (ΔC=C)	C–Cl (ΔC–Cl)	C=C–Cl (ΔC=C–Cl)
^1A_g	1.324	1.724	122.68
Expt.[b]	1.354	1.718	122.15
$^2B_{2u}$	1.422(+0.098)	1.670(−0.054)	120.85(−1.83)
$^2B_{2g}$	1.309(−0.015)	1.702(−0.022)	122.54(−0.14)
$^2B_{3u}$	1.317(−0.007)	1.722(−0.002)	126.74(+4.06)
^2A_u	1.319(−0.005)	1.716(−0.008)	122.72(+0.04)
$^2B_{1u}$	1.309(−0.015)	1.730(+0.006)	118.67(−4.01)
$^2B_{1g}$	1.324(−0.000)	1.724(+0.001)	123.93(+1.25)
^2A_g	1.375(+0.051)	1.707(−0.017)	121.42(−1.26)
$^2B_{3g}$	1.311(−0.013)	1.750(+0.026)	121.54(−1.14)

[a]Bond lengths are in angstroms, angles in degrees. The values in parentheses are the magnitude of the change in geometry by ionization.
[b]Reference 10.

TABLE II. Vibrational frequencies (cm^{-1}).

State	ν_1	ν_2	ν_3
^1A_g	1825	477	254
Obs.[a]	1571	447	237
$^2B_{2u}$	1531	507	271
$^2B_{2g}$	1900	488	206
$^2B_{3u}$	1875	478	252
^2A_u	1848	481	242
$^2B_{1u}$	1893	476	254
$^2B_{1g}$	1824	477	252
^2A_g	1449	483	275
$^2B_{3g}$	1880	466	245

[a]Reference 11.

TABLE III. Conventional potential energy distribution (%).

State	Component	ν_1	ν_2	ν_3
	ΔC=C	81.3	7.1	1.8
^1A_g	ΔC–Cl	11.7	91.5	1.1
	ΔC=C–Cl	7.0	1.5	97.1
	ΔC=C	71.4	13.2	3.7
$^2B_{2u}$	ΔC–Cl	17.5	82.9	1.2
	ΔC=C–Cl	11.1	3.9	95.2
	ΔC=C	83.9	8.1	1.0
$^2B_{2g}$	ΔC–Cl	11.7	91.3	0.4
	ΔC=C–Cl	4.4	0.7	98.6
	ΔC=C	80.1	8.9	2.1
$^2B_{3u}$	ΔC–Cl	13.8	89.3	1.8
	ΔC=C–Cl	6.1	1.9	96.1
	ΔC=C	81.9	7.4	1.6
^2A_u	ΔC–Cl	11.9	91.3	0.9
	ΔC=C–Cl	6.2	1.2	97.5
	ΔC=C	84.4	5.7	1.1
$^2B_{1u}$	ΔC–Cl	8.6	93.6	0.1
	ΔC–C–Cl	7.1	0.7	98.8
	ΔC=C	81.1	7.2	1.7
$^2B_{1g}$	ΔC–Cl	12.2	91.3	1.3
	ΔC=C–Cl	6.8	1.5	97.0
	ΔC=C	76.1	5.0	0.1
^2A_g	ΔC–Cl	13.5	92.3	4.7
	ΔC=C–Cl	10.5	2.7	95.1
	ΔC=C	83.5	6.5	1.4
$^2B_{3g}$	ΔC–Cl	10.1	92.3	0.9
	ΔC=C–Cl	6.4	1.1	97.7

TABLE IV. Classical half-amplitude of the zero point vibrational levels.[a]

State	Component	ν_1	ν_2	ν_3
^1A_g	ΔC=C	0.055	0.007	0.003
	ΔC–Cl	−0.016	0.020	0.002
	ΔC=C–Cl	−0.8	−0.1	1.0
$^2B_{2u}$	ΔC=C	0.060	0.013	0.005
	ΔC–Cl	−0.017	0.018	0.002
	ΔC=C–Cl	−0.9	−0.3	0.9
$^2B_{2g}$	ΔC=C	0.054	0.008	0.002
	ΔC–Cl	−0.015	0.020	0.001
	ΔC=C–Cl	−0.8	−0.1	1.1
$^2B_{3u}$	ΔC=C	0.055	0.008	0.003
	ΔC–Cl	−0.017	0.020	0.002
	ΔC=C–Cl	−0.7	−0.2	1.00
^2A_u	ΔC=C	0.055	0.008	0.003
	ΔC–Cl	−0.016	0.020	0.001
	ΔC=C–Cl	−0.8	−0.2	1.0
$^2B_{1u}$	ΔC=C	0.054	0.006	0.002
	ΔC–Cl	−0.014	0.021	0.000
	ΔC=C–Cl	−0.8	−0.1	1.0
$^2B_{1g}$	ΔC=C	0.055	0.008	0.003
	ΔC–Cl	−0.016	0.020	0.002
	ΔC=C–Cl	−0.8	−0.2	1.0
^2A_g	ΔC=C	0.062	0.007	0.001
	ΔC–Cl	−0.017	0.020	0.004
	ΔC=C–Cl	−0.9	−0.2	1.0
$^2B_{3g}$	ΔC=C	0.055	0.007	0.002
	ΔC–Cl	−0.015	0.021	0.001
	ΔC=C–Cl	−0.8	−0.1	1.0

[a]Bond lengths are in angstroms, angles in degrees.

tions are about 0.055 Å, 0.020 Å, and 1.0°, respectively. Comparing these values with the change in the equilibrium molecular structure, we find some significant changes. The magnitudes of the change in the C=C, C–Cl distances and the C=C–Cl angle of the $^2B_{2u}$ state are larger than those of the classical half-amplitude. We also find that the change in the C=C–Cl angle of the $^2B_{3u}$ and $^2B_{1u}$ states are larger than the magnitudes of the classical half-amplitude by four times. The changes in the C=C of ^2A_g, C–Cl of $^2B_{2g}$ and $^2B_{3g}$, and C=C–Cl of $^2B_{1g}$, ^2A_g, and $^2B_{3g}$ are the same order. The changes in the geometric parameters of the ^2A_u state are smaller than the magnitudes of the classical half-amplitude. Table II shows the vibrational frequencies of the ionic states. It is found from Tables III and IV that the characters of the ν_1, ν_2, and ν_3 modes of all states correspond generally to those of the ground state. We notice that some obvious changes of frequencies are found in the ν_1 mode of the $^2B_{2u}$ and ^2A_g states. The frequencies decrease. This should be connected so that the C–Cl distance lengthens by ionization.

Table V shows the VI and AI energies at the SCF and SDCI levels. In the SDCI calculations, the weights of the reference function are 82%–83% at the optimized geometry. Table V shows the energy lowering of the AI energy compared with the VI energy. A large energy lowering is found in the $^2B_{2u}$ state corresponding to the large change in the equilibrium molecular structure, while the energy lowering of the $^2B_{2g}$, ^2A_u, and $^2B_{1g}$ states are negligibly small. Within the short range of 0.8 eV, we find the five ionic states: $^2B_{3u}$, ^2A_u, $^2B_{1u}$, $^2B_{1g}$, and ^2A_g. The ordering of the states is different using either VI or AI energies. We notice that the VI energy of the $^2B_{3u}$ state is lower than that of the ^2A_u state, while the AI energy of $^2B_{3u}$ is larger than that of the ^2A_u state. It is also noticed that the order of the $^2B_{1u}$ and $^2B_{1g}$ states changes by using either VI or AI energies. This situation is connected so that the lowerings of the AI energy from the VI energy of the ^2A_u and $^2B_{1g}$ states are negligibly small, while those of the $^2B_{3u}$ and $^2B_{1u}$ states are larger than the differences of the VI energies between the $^2B_{3u}$ and ^2A_u states, and between the $^2B_{1u}$ and $^2B_{1g}$ states, respectively. The 0–0 ionization energies and the FCFs of the 0–0 transitions are listed in Table V. The FCFs of the $^2B_{2u}$, $^2B_{2g}$, ^2A_u, $^2B_{1g}$, ^2A_g, and $^2B_{3g}$ states are so large that the 0–0 transitions should be observed. Lake and Thompson reported that the observed 0–0 band of the first band was 9.34 eV. The present calculated value is underestimated by 0.55 eV in comparison with their value.

The total feature of the theoretical intensity curves of the $^2B_{2u}$, $^2B_{2g}$, $^2B_{3u}$, ^2A_u, $^2B_{1u}$, $^2B_{1g}$, ^2A_g, and $^2B_{3g}$ states are illustrated in Fig. 2 by assuming a half-width of 0.08 eV for each transition band. It is compared with the observed PE spectrum by Kimura *et al.*[2] It imitates well the shape of the observed PE spectrum. To discuss more detailed vibrational structure of each band and the contribution of each band to the spectrum, we illustrate the theoretical intensity curve

TABLE V. Ionization energies (eV).[a]

	VIE		AIE		Δ(VIE–AIE)		0–0 transition	
State	SCF	SDCI	SCF	SDCI	SCF	SDCI	0–0 IE	FCF
$^2B_{2u}$	9.02	9.23	8.61	8.81	0.41	0.42	8.79	0.072
$^2B_{2g}$	11.83	11.49	11.79	11.48	0.04	0.01	11.48	0.479
$^2B_{3u}$	12.88	12.53	12.63	12.30	0.25	0.23	12.30	0.000
^2A_u	12.79	12.40	12.79	12.40	0.00	0.00	12.40	0.915
$^2B_{1u}$	13.26	12.88	12.99	12.61	0.27	0.27	12.61	0.000
$^2B_{1g}$	13.18	12.77	13.16	12.76	0.02	0.01	12.76	0.475
^2A_g	13.48	13.11	13.41	13.01	0.07	0.10	12.99	0.573
$^2B_{3g}$	14.12	13.72	14.04	13.64	0.08	0.08	13.64	0.241

[a]Total energies (a.u.) of ^1A_g: −1911.569 329 (SCF) and −1912.238 285 (SDCI). VIE: Vertical ionization energy; AIE: adiabatic ionization energy.

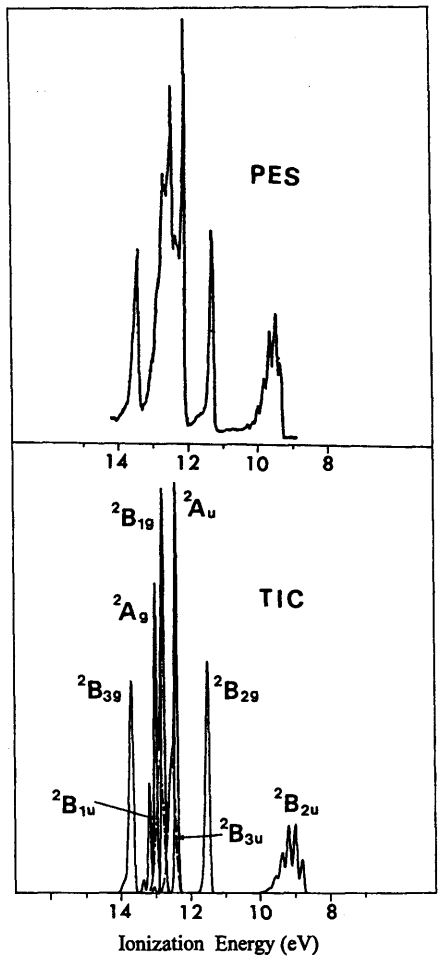

FIG. 2. The total feature of the theoretical intensity curve of ionization with a half-width of 0.08 eV and the observed photoelectron spectrum by Kimura *et al.* (Ref. 2). TIC: Theoretical intensity curve; PES: PE spectrum.

TABLE VI. Vibrational levels of the $^2B_{2u}$ state.

	Progressions		
IE	*A*	*B*	*C*
8.79	*M*(0 0 0)[a]		
8.85		*M*(0 1 0)	
8.92			*W*(0 2 0)
8.98	*S*(1 0 0)		
9.04		*S*(1 1 0)	
9.11			*W*(1 2 0)
9.17	*S*(2 0 0)		
9.23		*S*(2 1 0)	
9.29			*W*(2 2 0)
9.36	*M*(3 0 0)		
9.42		*M*(3 1 0)	
9.48			*W*(3 2 0)
9.55	*W*(4 0 0)		
9.61		*W*(4 1 0)	
9.67			*W*(4 2 0)
9.74	*W*(5 0 0)		
9.80		*W*(5 1 0)	

[a]Intensity is classified into *S*, *M*, or *W* according to the magnitude of FCF as follows: *S*:0.15>FCF>0.08; *M*:0.08>FCF>0.03; or *W*:0.03>FCF <0.007.

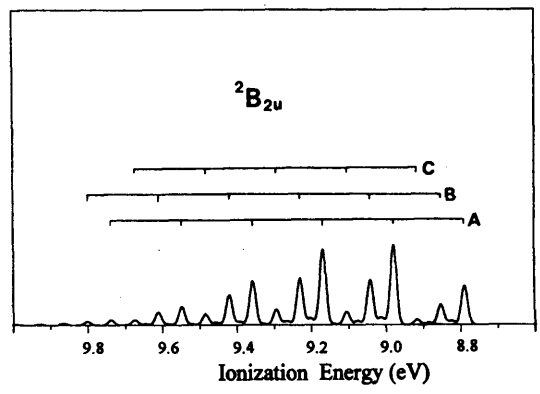

FIG. 3. The theoretical intensity curve of ionization of the $^2B_{2u}$ state with a half-width of 0.02 eV.

with a half-width of 0.02 eV. The results are shown in Figs. 3 to 10. The assignments of the vibrational structures are found in the figures or Tables VI to X.

Figure 3 illustrates the theoretical intensity curve of the $^2B_{2u}$ state. A well resolved vibrational structure is found. Three vibrational progressions of *A*, *B*, and *C* are recognized. An assignment of each progression is found in Table VI. The progression *A* with strong intensity is a series of vibrational excitations of (0 0 0)–(5 0 0). The progression *B* with medium intensity is a series of (0 1 0)–(5 1 0) and the progression *C* with weak intensity is a series of (0 2 0)–(4 2 0). Lake and Thompson reported the observed frequencies of 1320 and 484 cm^{-1}, which were assigned as the C=C and C–Cl stretching modes, respectively. The present calculated frequencies of the ν_1 and ν_2 modes are 1531 and 507 cm^{-1}, respectively. The calculated values overestimate by 16.0% and 4.8% in comparison with their values. The vibrational excitations of the ν_1 mode have a strong intensity. This situation is connected to the change in the geometry. It is found from Table I that the C=C bond becomes long, the C–Cl bond becomes short, and the C=C–Cl angle becomes nar-

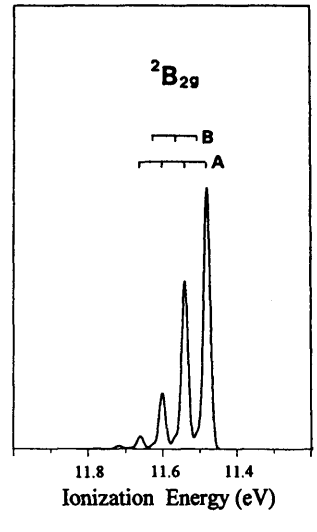

FIG. 4. The theoretical intensity curve of ionization of the $^2B_{2g}$ state with a half-width of 0.02 eV.

TABLE VII. Vibrational levels of the $^2B_{2g}$ state.

IE	Progressions	
	A	*B*
11.48	*S*(0 0 0)[a]	
11.51		*M*(0 0 1)
11.54	*S*(0 1 0)	
11.57		*W*(0 1 1)
11.60	*S*(0 2 0)	
11.63		*W*(0 2 1)
11.66	*W*(0 3 0)	

[a]Intensity is classified into *S*, *M*, or *W* according to the magnitude of FCF as follows: *S*:0.48>FCF<0.10; *M*:0.04>FCF>0.03; or *W*:0.03>FCF >0.008.

row. The magnitude of the change is larger than that of the classical half-amplitude of the zero point vibrational level. The main character of the ν_1 mode is the C=C stretching motion, but it is found from Table IV that the C–Cl stretching and C=C–Cl bending motions mix and that the phase of the motion is consistent with that of the change in the geometry by ionization. Thus, higher vibrational excitations of the ν_1 mode become important.

Figure 4 shows the theoretical intensity curve of the $^2B_{2g}$ state. It shows that the 0–0 transition has the maximum transition probability. Therefore, the observed VI energy of 11.38 eV should correspond to the 0–0 transition energy. The calculated value is 11.48 eV, which overestimates by 0.10 eV. The two vibrational progressions are found in Fig. 4. The assignment is given in Table VII. The progression with strong intensity is the (0 0 0)–(0 3 0) transition. It is found from Tables I and IV that the magnitude of the geometrical change in the C–Cl length is the same order as that of the classical half-amplitude of the zero point vibrational level. Thus, the lower vibrational excitations of the ν_2 mode contribute to the intensity.

In the 12–13 eV region, Lake and Thompson observed the six peaks at 12.18, 12.44, 12.54, 12.67, 12.77, and 12.91 eV. The present calculation suggests that the $^2B_{3u}$, ^2A_u, $^2B_{1u}$, $^2B_{1g}$, and ^2A_g states contribute to the spectrum in this region. The theoretical intensity curves illustrated from Figs. 5–9 shows that the 0–0 transition of the ^2A_u, $^2B_{1g}$, and ^2A_g states have the maximum transition probability. Therefore, it

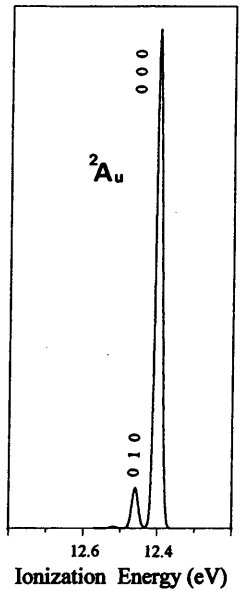

FIG. 6. The theoretical intensity curve of ionization of the ^2A_u state with a half-width of 0.02 eV.

should be reasonable to assign the observed peak to some of these 0–0 transition states. We propose that the peaks at 12.18, 12.54, and 12.77 eV should correspond to the 0–0 transition of the ^2A_u, $^2B_{1g}$, and ^2A_g states, respectively. The calculated 0–0 energies are 12.40, 12.76, and 12.99 eV, which values overestimate equally by 0.22 eV. Figure 6 shows that the (0 1 0) level of the ^2A_u state is medium intensity. The frequency corresponding to the spacing of the observed 12.18 and 12.44 eV is 2097 cm^{-1}. We could not assign the peak at 12.44 eV to the (0 1 0) level of the ^2A_u state, because the calculated frequency of the ν_2 mode is 481 cm^{-1} which is very small compared to the observed spacing. It is found from Fig. 8 that the (0 0 1) level of the $^2B_{1g}$ state is of strong intensity. The frequency corresponding to the spacing of the observed 12.76 and 12.67 eV is 1049 cm^{-1}. We also could not assign the peak at 12.67 eV to the (0 0 1) level of the $^2B_{1g}$ state, because the calculated frequency of the ν_3 mode is 252 cm^{-1} which is very small compared to the observed spacing. Figure 9 shows that the (1 0 0) level of

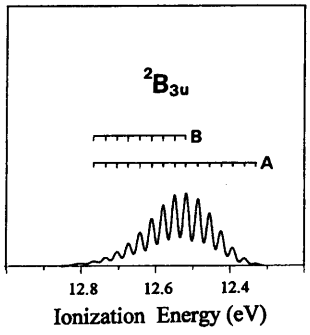

FIG. 5. The theoretical intensity curve of ionization of the $^2B_{3u}$ state with a half-width of 0.02 eV.

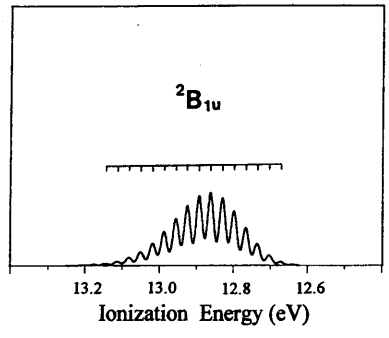

FIG. 7. The theoretical intensity curve of ionization of the $^2B_{1u}$ state with a half-width of 0.02 eV.

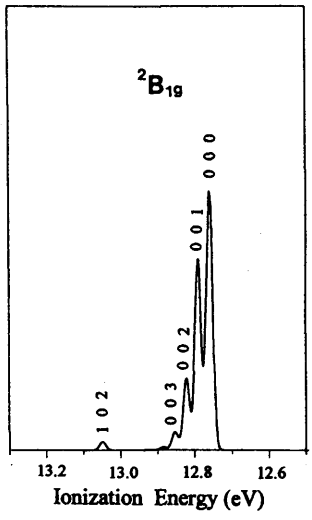

FIG. 8. The theoretical intensity curve of ionization of the $^2B_{1g}$ state with a half-width of 0.02 eV.

TABLE VIII. Vibrational levels of the $^2B_{3u}$ state.

IE	Progressions	
	A	*B*
12.33	*W*(0 0 1)[a]	
12.36	*W*(0 0 2)	
12.39	*M*(0 0 3)	
12.43	*M*(0 0 4)	
12.45–12.46	*S*(0 0 5)	*W*(0 1 3)
12.48–12.49	*S*(0 0 6)	*W*(0 1 4)
12.51–12.52	*S*(0 0 7)	*W*(0 1 5)
12.55	*S*(0 0 8)	*W*(0 1 6)
12.58	*S*(0 0 9)	*W*(0 1 7)
12.61	*M*(0 0 10)	*W*(0 1 8)
12.64	*M*(0 0 11)	*W*(0 1 9)
12.67–12.68	*W*(0 0 12)	*W*(0 1 10)
12.70–12.71	*W*(0 0 13)	*W*(0 1 11)
12.73–12.74	*W*(0 0 14)	*W*(0 1 12)

[a]Intensity is classified into *S*, *M*, or *W* according to the magnitude of FCF as follows: *S*: 0.11>FCF>0.08; *M*:0.07>FCF>0.03; or *W*: 0.03>FCF >0.003.

the ^2A_g state is of strong intensity. The frequency corresponding to the spacing of the observed 12.77 and 12.91 eV is 1130 cm^{-1}. We should assign the peak at 12.91 eV to the (1 0 0) level of the ^2A_g state, because the calculated frequency of the ν_1 mode is 1449 cm^{-1} which corresponds to the observed spacing. The theoretical intensity curves of the $^2B_{3u}$ and $^2B_{1u}$ states are illustrated in Figs. 5 and 7, respectively. It shows a broad and similar vibrational structure. It is found from the figures that the peaks with the maximum intensity of the $^2B_{3u}$ and $^2B_{1u}$ states are 12.55 and 12.86 eV, respectively. We therefore propose the assignment that the observed peaks at 12.44 and 12.67 eV should correspond to the peaks with the maximum intensity of the $^2B_{3u}$ and $^2B_{1u}$ states, respectively. We notice that the calculated VI energies of the $^2B_{3u}$ and $^2B_{1u}$ states (11.53 and 11.88 eV) does not correspond to the energies with the maximum intensity of these states.

The theoretical intensity curves of the ^2A_u, $^2B_{1g}$, and ^2A_g states are illustrated in Figs. 6, 8 and 9, respectively. It shows a very sharp vibrational structure. This feature is connected to the small change in the geometrical parameters by ionization. It is found from Tables I and IV that each magnitude of the change is smaller or the same level compared to that of the classical half-amplitude. Therefore, the intensity of the 0–0 transition is the largest of all and only the lower vibrational excitations contribute to the intensity. The theoretical intensity curves of the $^2B_{3u}$ and $^2B_{1u}$ states shows a broad and similar vibrational structure. The assignments of the vibrational structures are found in Tables VIII and IX. It is found from the tables that the higher vibrational excitations of the ν_3 mode contribute to the intensity. This situation is ascribed to the large geometrical change in the C═C–Cl

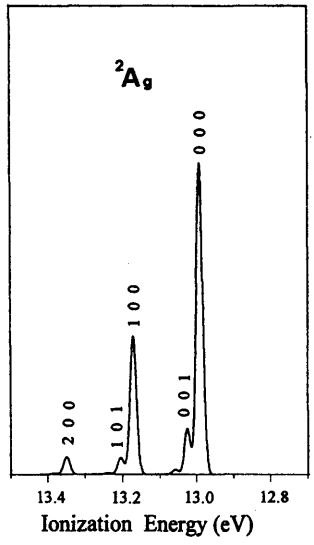

FIG. 9. The theoretical intensity curve of ionization of the ^2A_g state with a half-width of 0.02 eV.

TABLE IX. Vibrational levels of the $^2B_{1u}$ state.

IE	Progression *A*
12.64	*W*(0 0 1)[a]
12.67	*W*(0 0 2)
12.70	*W*(0 0 3)
12.74	*M*(0 0 4)
12.77	*M*(0 0 5)
12.80	*S*(0 0 6)
12.83	*S*(0 0 7)
12.86	*S*(0 0 8)
12.89	*S*(0 0 9)
12.92	*S*(0 0 10)
12.96	*S*(0 0 11)
12.99	*M*(0 0 12)
13.02	*M*(0 0 13)
13.05	*W*(0 0 14)
13.08	*W*(0 0 15)
13.11	*W*(0 0 16)

[a]Intensity is classified into *S*, *M*, or *W* according to the magnitude of FCF as follows: *S*: 0.13>FCF>0.08; *M*: 0.07>FCF>0.03; or *W*: 0.03>FCF >0.001.

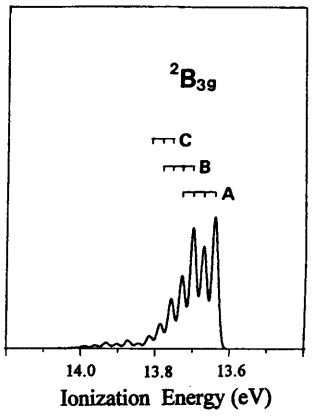

FIG. 10. The theoretical intensity curve of ionization of the $^2B_{3g}$ state with a half-width of 0.02 eV.

bond angles of both states. The magnitudes of the changes are equal to each other and four times as large compared to the classical half-amplitude of the zero point vibrational level. Therefore, very similar vibrational structures with higher excitations of the ν_3 mode should appear.

Figure 10 shows the theoretical intensity curves of the $^2B_{3g}$ state. It shows that the 0–0 transition is the maximum intensity. Therefore, the observed ionization energy of 13.48 eV should be interpreted as the 0–0 ionization energy of the $^2B_{3g}$ state. The calculated 0–0 ionization energy is 13.64 eV, which overestimates by about 0.16 eV in comparison with the observed value. Figure 10 shows the three vibrational progressions. The assignment of the progressions is given in Table X. The progressions of (0 0 0)–(0 0 3) and (0 1 0)–(0 1 3) have strong intensity. Lake and Thompson reported that the observed spacing of 460 cm^{-1} was assigned to the C–Cl stretching mode. It is found from Fig. 10 that the first and third peaks have strong intensity and the frequency of this spacing corresponds to that of the ν_2 and $2\nu_3$ transitions. The calculated frequencies of the ν_2 and $2\nu_3$ transitions are 466 and 490 cm^{-1}, respectively. We, therefore, propose that the observed frequency of 460 cm^{-1} should be assigned to the frequency of the ν_2 and $2\nu_3$ transitions. It is found from Tables I and IV that the magnitude of the change in the C–Cl length and C=C–Cl angle is the same level as that of the classical half-amplitude. Thus, the intensity of the 0–0 transition is the largest of all and only the lower vibrational excitations of the ν_2 and ν_3 modes contribute to the intensity.

TABLE X. Vibrational levels of the $^2B_{3g}$ state.

	Progressions		
IE	*A*	*B*	*C*
13.64	*S*(0 0 0)[a]		
13.67	*S*(0 0 1)		
13.70	*M*(0 0 2)	*S*(0 1 0)	
13.73	*W*(0 0 3)	*S*(0 1 1)	
13.76		*M*(0 1 2)	*M*(0 2 0)
13.79		*W*(0 1 3)	*M*(0 2 1)
13.82			*W*(0 2 2)

[a]Intensity is classified into *S*, *M*, or *W* according to the magnitude of FCF as follows: *S*: 0.24>FCF>0.08; *M*: 0.08>FCF>0.03; or *W*: 0.03>FCF >0.009.

Kimura *et al.* have reported the calculated vertical ionization energies by using the Koopmans' theorem with the 4-31G basis set. They have assigned the first and second bands as to the $^2B_{3u}$ and $^2B_{3g}$ states, respectively. Niessen *et al.*[3] have obtained the same assignment. Their assignments appear to be different from the present assignment. This is connected to the arbitrariness of the choice of the coordinate axis. If we change the x axis by the y axis in Fig. 1, we obtain the same assignment. The a_g, b_{1g}, b_{2g}, b_{3g}, a_u, b_{1u}, b_{2u}, and b_{3u} MOs of the present coordinate axis are correlated to the a_g, b_{1g}, b_{3g}, b_{2g}, a_u, b_{1u}, b_{3u}, and b_{2u} MOs of their coordinate axis, respectively. It is found from the calculation by Kimura *et al.* that the electronic configuration of the ground state is a $...(2b_{1g})^2(10a_g)^2(10b_{2u})^2(2b_{2g})^2(7b_{1u})^2(2a_u)^2(5b_{3g})^2(4b_{3u})^2$. Their numbering and characterization of the MO should be missed. The total electron of the ground state is 80 but their configuration gives 84 electrons. Using their coordinate axis, we get the configuration of $...(2b_{2g})^2(9a_g)^2(8b_{1u})^2(2b_{1g})^2(7b_{2u})^2(2a_u)^2(7b_{3g})^2(3b_{3u})^2$.

IV. CONCLUSIONS

The molecular equilibrium structures and vibrational frequencies are calculated for the ground state of ^1A_g and the lower eight ionic states of $^2B_{2u}$, $^2B_{2g}$, ^2A_u, $^2B_{3u}$, $^2B_{1g}$, ^2A_g, $^2B_{1u}$, and $^2B_{3g}$. Using the FCFs, we obtain the theoretical intensity curve. The theoretical intensity curve is in good agreement with the observed PE spectrum.

The main characters of the ν_1, ν_2, and ν_3 modes of the ground state are C=C stretching, the C–Cl stretching, and C=C–Cl bending motions, respectively. The characters of the vibrational modes of all ionic states correspond generally to those of the ground state.

The first peak observed at 9.34 eV should be assigned to the 0–0 ionization energy of the $^2B_{2u}$ state and the vibrational excitation of the ν_1 mode contributes to the vibrational structure. Although the main character of the ν_1 mode is the C=C stretching motion, the C–Cl stretching and C=C–Cl bending motions mix and the phase of the motion is consistent with that of the change in the geometry by ionization: the C=C bond becomes long, the C–Cl bond becomes short, and the C=C–Cl angle becomes narrow.

The second band should be assigned to the $^2B_{2g}$ state. The vibrational excitation of the C–Cl stretching mode of ν_2 contributes to the intensity.

In the 12–13 eV region, the peaks at 12.18, 12.44, 12.54, 12.67, 12.77, and 12.91 eV were reported. We propose the assignment that the peaks at 12.18, 12.54, and 12.77 eV should correspond to the 0–0 transitions of the ^2A_u, $^2B_{1g}$, and ^2A_g states, respectively. The peaks at 12.44 and 12.67 eV should be the peaks with the maximum intensity of the $^2B_{3u}$ and $^2B_{1u}$ states, respectively. The peak at 12.91 eV should be

the (1 0 0) level of the ^2A_g state. The shapes of the vibrational structures of the ^2A_u and $^2B_{1g}$ states are very sharp. This situation is connected to the small geometrical change by ionization. The vibrational structures of the $^2B_{3u}$ and $^2B_{1u}$ states are broad and the higher vibrational excitations of the ν_3 mode contribute to the intensity. This is ascribed to the large geometrical change in the C=C–Cl angle. The magnitude of change is four times as large compared to the classical half-amplitude of the zero point vibrational level. The change in the C=C length of the ^2A_g state is the same order as the classical half-amplitude. Thus the vibrational excitation to the (1 0 0) level also has strong intensity.

The observed peak at 13.48 eV should be the 0–0 ionization transition of the $^2B_{3g}$ state. The observed frequency of 460 cm^{-1} should correspond to the frequency of the ν_2 and $2\nu_3$ transitions. The magnitude of the changes in the C–Cl length and C=C–Cl angle is the same level as those of the classical half-amplitude Therefore the 0–0 transition is the largest of all and only the lower vibrational excitations of the ν_2 and ν_3 modes contribute to the intensity.

ACKNOWLEDGMENT

Computation was carried out on HITAC M-680H systems at the Center for Information Processing Education of Hokkaido University.

[1] R. F. Lake and H. Thompson, Proc. R. Soc. London Ser. A **315**, 323 (1970).
[2] K. Kimura, S. Katsumata, Y. Achiba, T. Yamazaki, and S. Iwata, *Handbook of HeI Photoelectron Spectra of Fundamental Organic Molecules* (Halsted, New York, 1981).
[3] W. V. Niessen, L. Åsbrink, and G. Bieri, J. Electron Spectrosc. Relat. Phenom. **26**, 173 (1982).
[4] H. Tatewaki and S. Huzinaga, J. Comput. Chem. **1**, 205 (1980).
[5] A. D. Mclean and B. Liu, J. Chem. Phys. **58**, 1066 (1973).
[6] T. Shoda, T. Noro, T. Nomura, and K. Ohno, Int. J. Quantum Chem. **30**, 289 (1986).
[7] K. Takeshita, J. Chem. Phys. **86**, 329 (1987).
[8] K. Takeshita and F. Sasaki, 1981 Library program at the Hokkaido University Computing Center (in Japanese). GRAMOL included the Program JAMOL3 of the RHF calculation written by H. Kashiwagi, T. Takada, E. Miyoshi, and S. Obara for the Library program at the Hokkaido University Computing Center 1977 (in Japanese).
[9] A. Murakami, H. Iwaki, H. Terashima, T. Shoda, T. Kawaguchi, and T. Noro, 1986 Library program at the Hokkaido University Computing Center (in Japanese).
[10] T. G. Strand, Acta Chem. Scand. **21**, 2111 (1967).
[11] G. Herzberg, *Molecular Spectra and Molecular Structure, Part III* (Van Nostrand, New York, 1966).